NMR Spin Grouping

H. Peemoeller

Guelph-Waterloo Program for Graduate Work in Physics
Department of Physics
University of Waterloo
Waterloo, Ontario, Canada, N2L 3G1

Contents

I. Introduction

NMR spectroscopy has been used extensively to study the structure and dynamics of heterogeneous systems. If spectroscopic lines do not overlap, the information about the various spin groups in the system can be found directly. However, in many heterogeneous systems spectroscopic lines overlap to such an extent that useful information about the individual spin groups cannot be obtained. Examples of such materials, which are of practical importance, include wood, cement pastes, oil sands, tissues and dense biopolymer solutions. As a consequence of the overlap of spectroscopic lines the molecular coordination and motion in these materials can not be studied with standard techniques.

Consider the response from a heterogeneous system upon excitation by a resonant r.f. pulse. A composite signal from various spin groups in different environments results. In order to gain insight into molecular coordination and motion of these spin groups it is essential to resolve and characterize the different spin groups with a set of NMR relaxation parameters. This necessitates the decomposition of the total (composite) NMR response into a sum of spin group responses. In section II a technique is discussed that in some cases allows such decomposition even for overlapping resonance lines. This technique is a form of two dimensional (2D) NMR (1) time evolution correlation spectroscopy called NMR Spin Grouping (2). The technique uses correlations between independent spectroscopic observations to resolve the overlap.

In many heterogeneous systems dynamical information cannot be obtained directly from NMR spin grouping due to exchange between individual spin groups. Such exchange may involve a physical exchange of nuclei bearing spins, or a magnetization transfer by energy conserving spin flips, or both. As a result of such exchange only apparent relaxation parameters (relaxation rates and magnetization fractions) are observed. The intrinsic (or true) parameters which contain information about molecular dynamics are not observed. However, by combining NMR spin grouping with selective excitation methods and exchange analysis, information about the intrinsic system NMR parameters as well as the exchange mechanism itself can be obtained. In section III the application of NMR spin grouping and exchange analysis to hydrated DNA is discussed.

II. NMR Spin Grouping Method

To illustrate the methodology involved in NMR spin grouping, consider a hypothetical sample with two uncoupled spin groups (a and b) in different environments for which the resonances overlap. Let the spin groups a and b have Gaussian line shapes with $T_{2a} = 20$ μs and $T_{2b} = 25$ μs. The corresponding T_1's are 10 ms and 100 ms. Spin groups a and b contribute 1/3 and 2/3 to the sample magnetization, respectively. The free induction decay (FID) following a $\pi/2$ pulse applied to such a sample at thermal equilibrium would appear as shown in Figure 1, where the normalized transverse magnetization is plotted against time t. M_0 is the sum of the spin group magnetizations at thermal equilibrium.

Experimentally the FID (Figure 1) appears to consist of a single Gaussian. As seen from the inset, in a typical experiment the decay curve would not be resolvable further as the plot $ln\ M_x(t)/M_0$ versus t^2 essentially is a straight line ($T_2 \sim 23$ μs).

Consider the result of a standard saturation recovery experiment performed on the sample in which the magnetization recovery is monitored at a time t = 10 μs along the FID; this is also referred to as a 10 μs "time window". In Figure 2 the magnetization recovery function $[M_0(t_1) - M_z(t_1, \tau)]/M_0(t_1)$ is plotted against τ, the spacing between the two pulses in the saturation recovery pulse sequence. Here $t_1 = 10$ μs and $M_0(t_1)$ is the sample magnetization at a 10 μs time window on the FID obtained following a $\pi/2$ pulse applied at thermal equilibrium. In this example the recovery function was found for 10 different τ values. In a typical experiment as many as 30 or more τ values may be used. The recovery curve is decomposed into two components (Figure 2); a component with long T_1 = 100 ms and M_0 (10 μs)/$M_0 \sim 2/3$ and a component with short T_1 = 10 ms and M_0 (10 μs)/$M_0 \sim$ 1/3. Although the standard spin-lattice relaxation experiment provides additional information it still leaves the spin groups unresolved; neither the T_2 nor the precise M_0 of each spin group was found.

The desired resolution is obtained by recording the magnetization evolution simultaneously at various times t along the FID for each value of τ. The recovery curve at each t is analysed using an interactive combination of statistical and graphical approaches (2). (i.e. decompositions as shown in Fig. 2 are performed at various times t.) This way, for each t, the value of T_{1i} and M_{0i} (t) for each resolvable component is obtained. A plot of the $\tau = 0$ intercepts M_{0i} (t) for each of the components gives the FIDs corresponding to the spin groups involved. For the present example, these intercepts are plotted in Figure 3 for 20 time windows. From the reconstructed transverse decay curves (Figure 3) two FIDs, corresponding to spin groups a and b, can be resolved; dashed line: a Gaussian with $T_{2a} = 20$ μs (T_{1a} = 10 ms and $M_{0a}/M_0 = 1/3$), solid line: a Gaussian with $T_{2b} = 25$ μs (T_{1b} = 100 ms and $M_{0b}/M_0 = 2/3$). In an experiment, each of the sets i of intercepts are fit to a Gaussian or exponential line shape. The t = 0 intercepts obtained from the fits to the reconstructed FIDs give the relative spin group sizes (M_{0i}/M_0). Thus, the spin groups have been resolved and characterized through their T_2, T_1 and M_0. As a typical experiment involves the determination of 30 or more T_1's for each spin group, a more representative T_{1i}, compared with standard pulse NMR experiments, is available through the average T_{1i}.

Spin grouping requires the decomposition of the nonexponential magnetization recovery function into separate exponentials. In order for this decomposition to be unambiguous, the component relaxation times must be sufficiently different ($\sim$ a factor 4 or more). If such difference is not observed in the high field experiments it may be necessary to study the 2D time evolution of the magnetization in the rotating frame and, if required, vary H_1 until the low field spin–lattice relaxation times ($T_{1\rho}$) differ enough to permit the accurate decomposition of the composite magnetization decay.

The main advantage offered by NMR spin grouping is that it gives improved spin group resolution compared with standard pulse NMR techniques. In addition, the technique lends itself to application of iteration approaches. For example, at each window along the FID the analysis of the magnetization recovery function yields T_1 values for each of the magnetization components. As T_1 of a particular magnetization component does not depend on t, the long T_1's are averaged to obtain the representative T_1 for this spin group. The analysis of each magnetization recovery function is then repeated by setting the T_1 of the component with long T_1 equal to the representative value at each time window t.

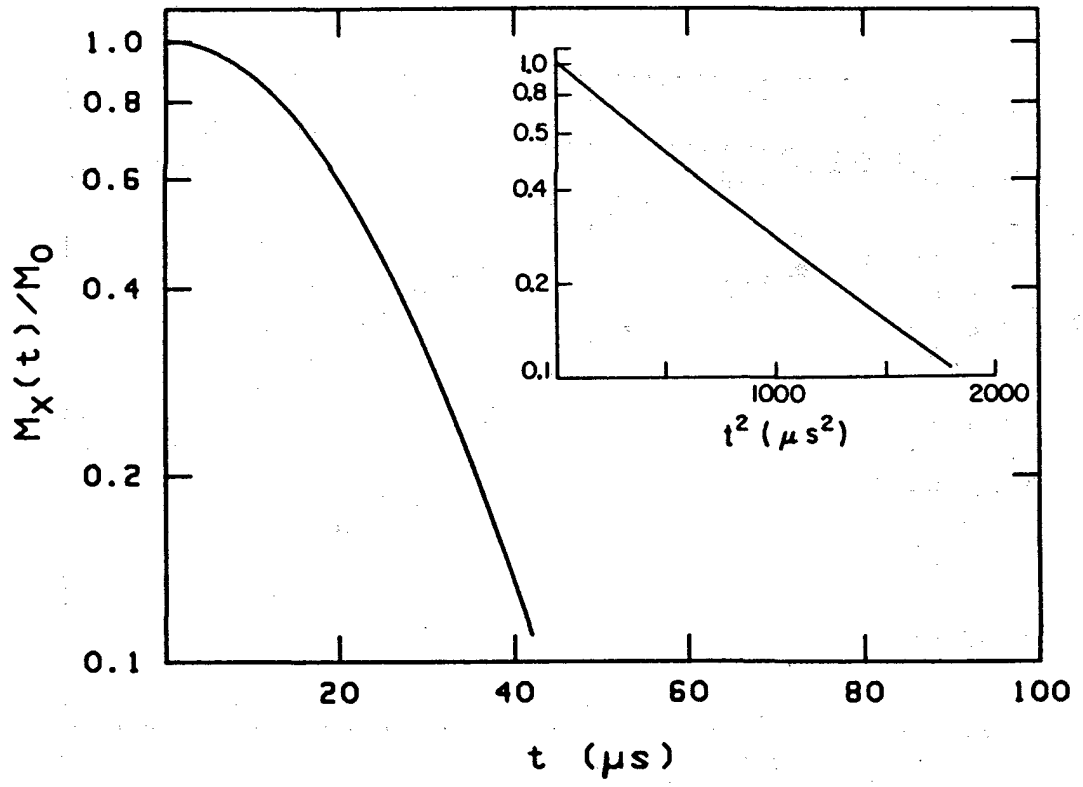

Figure 1. Composite FID of spin groups a and b. The inset shows a semi-logrithmic plot of normalized magnetization versus t^2.

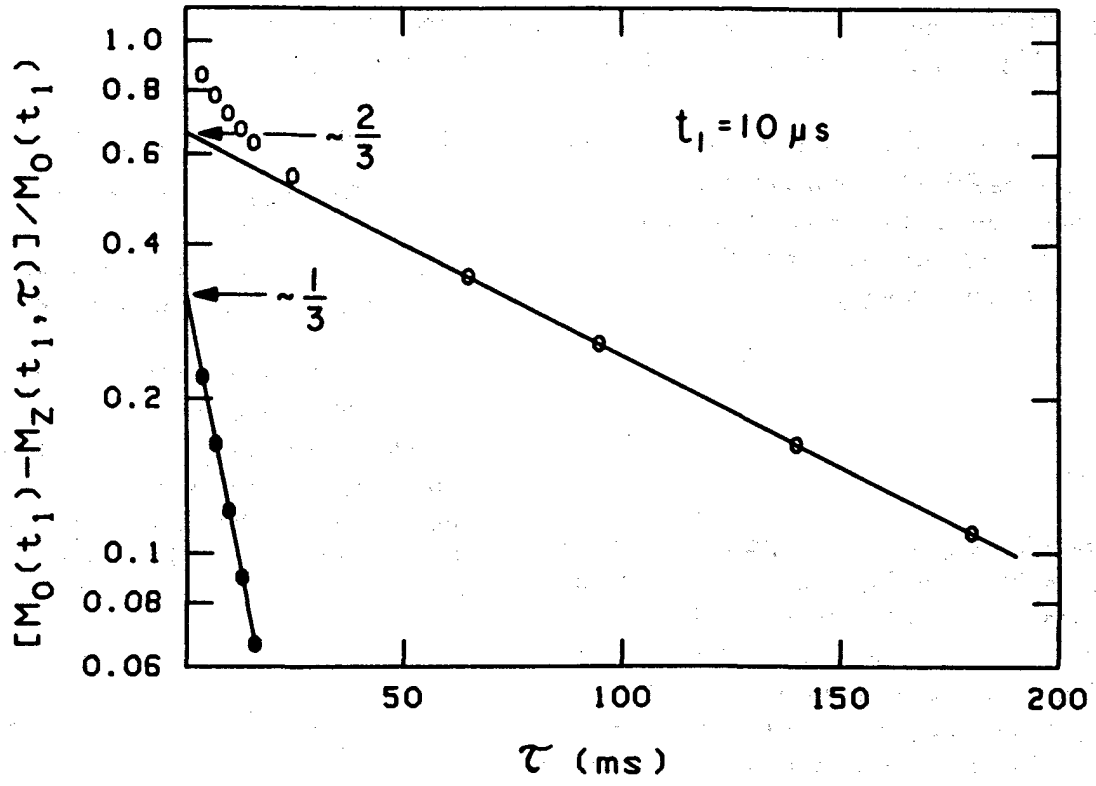

Figure 2. Magnetization recovery function at t = 10 μs for sample containing spin groups a and b.

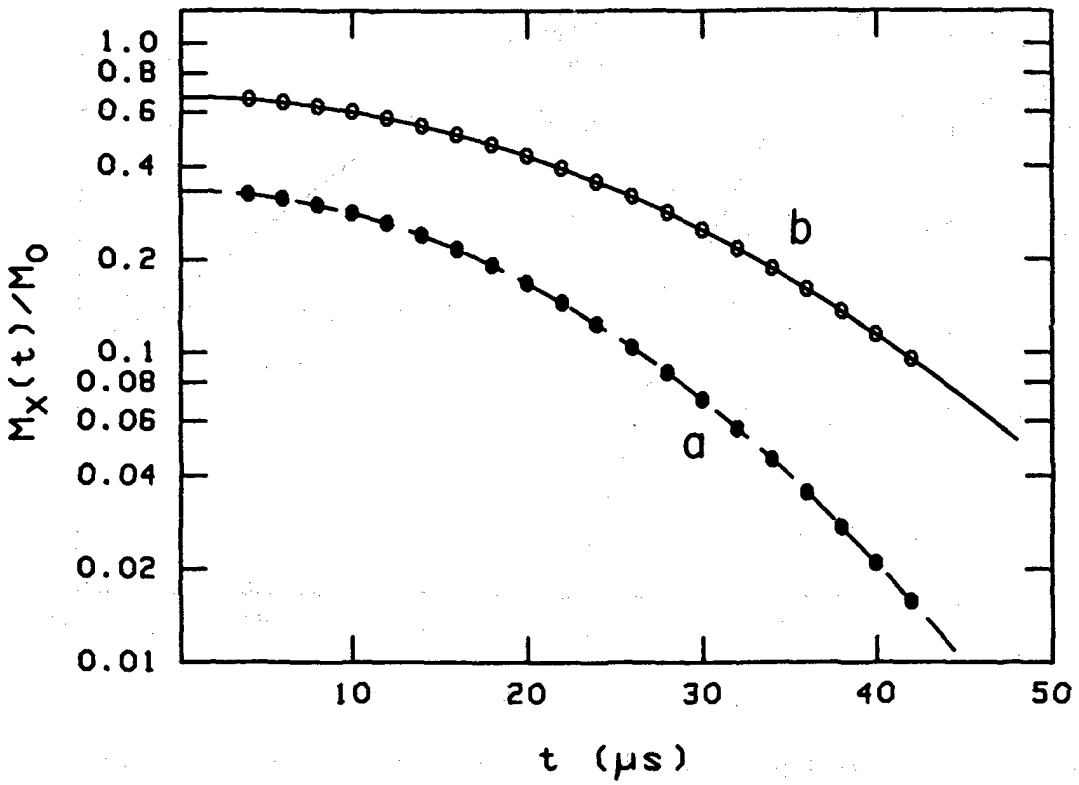

Figure 3. FID's reconstructed from spin-lattice relaxation results. Filled circles correspond to FID with T_1 = 10 ms and open circles correspond to FID with T_1 = 100 ms.

Such a re-analysis produces $\tau = 0$ intercepts which better define the FID of the magnetization with long T_1. The above procedure of incorporating representative T_1's into the analysis is repeated for each of the resolved components (3).

An iteration approach has recently been applied in which the T_1's (or $T_{1\rho}$'s) of the magnetization components are parameterized in a least-squares fitting routine. The routine proceeds through the decomposition at all time windows along the FID repeatedly, at each pass adjusting the component relaxation times until χ^2 has been reduced to the desired level. This approach works particularly well if the scatter in the raw data is small.

III. Spin Grouping and Exchange Analysis

A. Selective Excitation, Spin Grouping and Exchange in Hydrated Lysozyme

Consider a two phase system consisting of spin group a and spin group b.

The rates of magnetization exchange from group a to b (k_a) and from group b to a (k_b) are assumed nonzero. The evolution of the longitudinal magnetization is governed by the coupled differential equations

$$\frac{d[M_{0a} - M_{za}(\tau)]}{dt} = -(R_a + k_a)(M_{0a} - M_{za}) + k_b(M_{0b} - M_{zb}) \qquad (1)$$

$$\frac{d[M_{0b} - M_{zb}(\tau)]}{dt} = -(R_b + k_b)(M_{0b} - M_{zb}) + k_a(M_{0a} - M_{za}) \quad (2)$$

where R_a and R_b are the inherent or true relaxation rates of group a spins and group b spins, respectively. We assume that group a spins are in a solid with a Gaussian line shape (with second moment M_{2a}) and group b spins are in a liquid with a Lorentzian line shape (transverse relaxation time T_{2b}). For an inversion recovery sequence, the solution of the above coupled differential equations gives the following recovery function

$$F(t,\tau) = p_a m_a(\tau) e^{-M_{2a}t^2/2} + p_b m_b(\tau) e^{-t/T_{2b}} \quad (3)$$

where the effects of transverse magnetization decay have been explicitly included. The normalized z-magnetizations are given (4-6) by

$$m_{a,b}(\tau) = \frac{M_{0a,b} - M_{za,b}(\tau)}{2M_{0a,b}}$$

$$= C^+_{a,b} e^{-\lambda^+\tau} + C^-_{a,b} e^{-\lambda^-\tau} \quad (4)$$

where $\lambda^\pm$ are the apparent relaxation rates

$$2\lambda^\pm = (R_a + R_b + k_a + k_b) \pm \sqrt{(R_a - R_b + k_a - k_b)^2 + 4k_a k_b} \quad (5)$$

and coefficients $C^\pm_{a,b}$ have the form

$$C^\pm_{a,b} = \pm \frac{R_{a,b} - \lambda^\mp}{\lambda^+ - \lambda^-} m_{a,b}(0) \pm [m_{a,b}(0) - m_{b,a}(0)] \frac{k_{a,b}}{\lambda^+ - \lambda^-} \quad (6)$$

The fractions of spins in group a (p_a) and in group b (p_b) satisfy $p_a + p_b = 1$. In addition, the condition of detailed balance applies

$$k_a p_a = k_b p_b \quad (7)$$

In general, we wish to determine the intrinsic relaxation rates, the exchange rates and the sizes of the spin groups. This way the system can be characterized and information about molecular dynamics can be obtained. From eqn. (6) it is seen that both the exchange rates and the intrinsic relaxation rates can be found if the coefficients $C^\pm_{a,b}$ and rates $\lambda^\pm$ could be determined for two different initial conditions of the experiment (different $m_{a,b}(0)$). In fact, with the above, the spin populations p_a and p_b can also be calculated using eqn. (7). However, using standard NMR pulse approaches in the heterogeneous systems under consideration it generally is not possible to obtain the necessary coefficients and apparent relaxation rates for the following reasons. 1) Using standard NMR pulse experiments, all spin groups are excited equally so that the initial conditions are not variable. 2) Often the biopolymer-water system is in or near the fast exchange limit and as a consequence either no information or very limited information about the apparent rate λ^+ and the corresponding coefficients $C^+_{a,b}$ is available using standard NMR pulse experiments. For the most part we are interested in systems consisting of a solid-like spin group with a Gaussian FID ($T_2 \sim 10\ \mu s$) and a liquid-like spin group with an exponential FID having a T_2 of 1 ms or longer. In such systems the above difficulties can be circumvented with an experiment introduced (4) in 1978 that selectively excites the liquid-like and solid-like magnetizations. This approach involves an inversion recovery sequence with a selective or soft (S) preparation pulse and a nonselective or hard (H) monitor pulse. The values $m_{a,b}(0)$ can then be manipulated through the length t_p (and the amplitude B_1 of the r.f. field) of the preparation pulse. For example, if $t_p > M_2^{-1/2}$, where M_2 is the second moment of the resonance line of the solid-like spin group, and $t_p < T_2$ of the liquid-like magnetization then the liquid magnetization is inverted whereas the solid magnetization is not appreciably affected. 3) Standard NMR pulse techniques do not provide sufficient spin group resolution. Although selective excitation is a powerful approach for investigating the mixing of magnetizations of spin groups the difficulties depicted in section II are commonly encountered in these complex systems. As a consequence NMR spin grouping is essential in order to resolve the various magnetization components making up the composite response and in the process accurately define the corresponding sizes and relaxation times of spin groups.

NMR spin grouping combined with selective excitation, where the results are analysed for ex-

change (eqns. 1-7), was first applied (7) to hydrated lysozyme (178 mg H_2O/gram of sample). The FID in this sample consists of a Gaussian component with $T_2 \sim 15$ μs and an exponential component with $T_2 \sim 1.8$ ms. A good correspondence was found between the measured relative magnitudes of the Gaussian and exponential magnetization components and those calculated from the sample composition and spin densities of the water and lysozyme. This was taken as evidence that all of the protons in the sample are "seen" in the NMR experiment (7).

At a 100 μs time window long the FID, an exponential recovery curve was obtained using a HH inversion recovery sequence. However, employing a soft inverting pulse (SH inversion recovery sequence with $t_p = 80$ μs for the S-pulse) yields a two component recovery curve at the same time window. Figure 4 shows representative recovery curves at t = 100 μs (see Fig. 1 of reference 7). Because of its short T_2, the protein magnetization has dephased at the 100 μs time window. Thus, lines (a) and (b) in Fig. 4 are recovery curves for the water proton magnetization. The initial, rapid increase of water proton magnetization during the first 10 ms [line (b)] clearly shows the importance of magnetization transfer or cross-relaxation between the water protons and the lysozyme protons.

Figure 5 shows representative curves of the apparent magnetization fractions at $\tau = 0$ plotted as a function of t for a soft inverting pulse with $t_p = 80$ μs. On the basis of their T_2, the components a and b of the reconstructed FIDs (Fig. 5), obtained from the spin grouping analysis, are associated with protein protons and water protons, respectively. The t = 0 intercepts of the FIDs yield the coefficients $C^{\pm}_{a,b}$ (Fig. 5). A selective inversion experiment for which the soft inverting pulse has $t_p = 30\mu$s gave qualitatively the same results but with different values of $C^{\pm}_{a,b}$ (7). Using information about the known stoichiometry of the hydrated lysozyme sample and the values of $\lambda^{\pm}$ and $C^{\pm}_{a,b}$ obtained from the above spin grouping analysis eqn. (6) was solved for $k_{a,b}$ and the protein and water relaxation rates R_p and R_w (7).

The results were interpreted (7) in terms of an interfacial intermolecular cross-relaxation model in which on average all water protons interact with lysozyme protons with a cross-relaxation rate k. In this model the evolution of the magnetization is given by eqns. 1-6 but with k_a and k_b replaced with kf_w and kf_p, respectively. Here f_w and f_p are the respective fractions of water and protein protons directly coupled to each other. From the above results k = (98 $\pm$ 16) s^{-1}. $R_p = 6$ s^{-1} is approximately three times as large as the intrinsic protein proton spin-lattice relaxation rate R_{pi} measured in a dry lysozyme sample. Thus, the water–protein interaction not only results in spin-spin coupling and associated magnetization exchange effects, but also in lysozyme proton–water proton intermolecular spin–lattice relaxation. This relaxation rate R_{1wp} was estimated (7) at 8 s^{-1}. With this contribution taken into account the intrinsic water proton relaxation rate R_{wi} was calculated and analysed (7) for water molecule dynamics using standard relaxation equations (8). The resulting relaxation model for the hydrated lysozyme is summarized in Fig. 6.

B. Spin Grouping and Exchange Analysis in DNA

In the application to lysozyme the results from spin grouping were analysed for exchange by solving eqn. 6 for intrinsic and exchange parameters utilizing two different initial experimental conditions. Although such approach is straightforward, a more powerful approach that involves the correlation between results from several different experiments and utilizes simultaneous graphical displays of experimental and modelled intrinsic and exchange parameters has been developed recently (9-12).

This method referred to as NMR spin grouping and exchange analysis consists of the following four steps. First, a broad experimental basis is established using selective and nonselective pulses. Specifically HH T_1, SH T_1, SS T_1 and $T_{1\rho}$ experiments are performed. Second, spin grouping is applied to extract accurate values of $C^{\pm}_{a,b}$, $m_{a,b}$ (0) and $\lambda^{\pm}$ and to establish correlations between the results from different experiments. Such correlations improve the reliability of intrinsic relaxation parameters.

In the third step the results from spin grouping are analysed for exchange. To this end at least one of the populations $p_{a,b}$ is needed. In many cases the stoichiometry of the system will provide this information. In a binary liquid-solid system it may

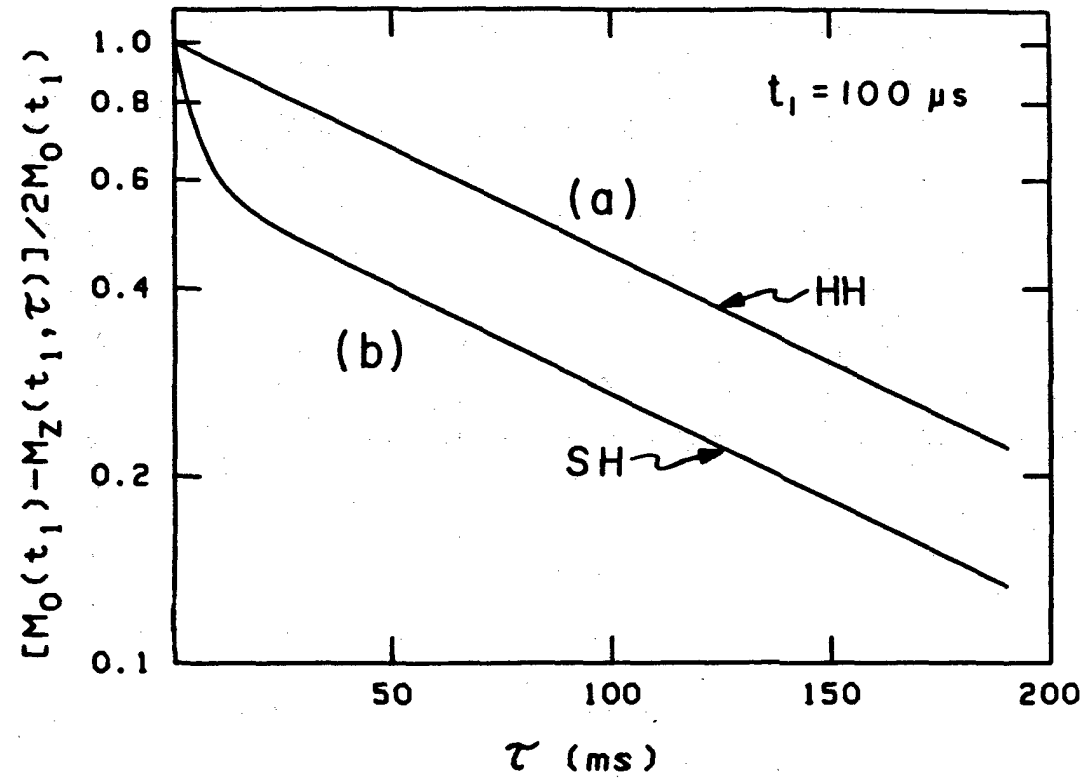

Figure 4. Recovery curves for hydrated lysozyme at t = 100 μs and (a) 180° pulse length = 3.2 μs; (b) 180° pulse length = 80 μs

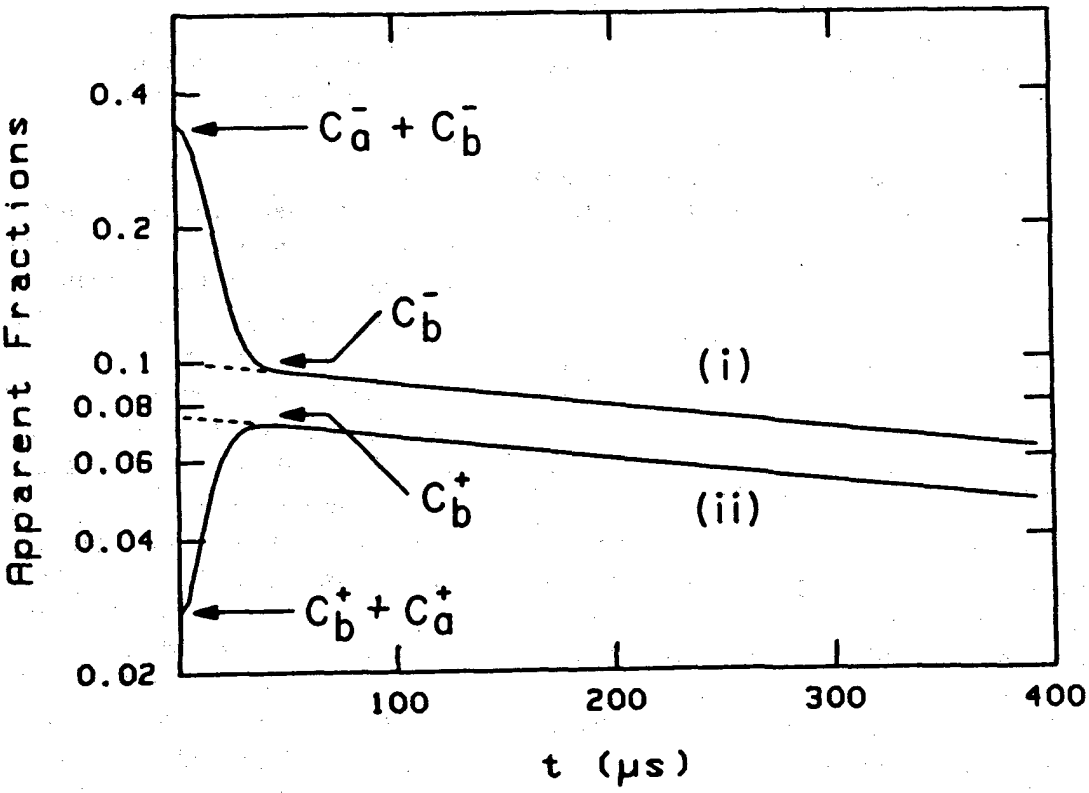

Figure 5. Apparent magnetization fractions at $\tau = 0$ versus t. Curve (i) is given by $C_a^- \exp(-M_{2a}t^2/2) + C_b^- \exp(-t/T_{2b})$ and (ii) by $C_a^+ \exp(-M_{2a}\, t^2/2) + C_b^+ \exp(-t/T_{2b})$.

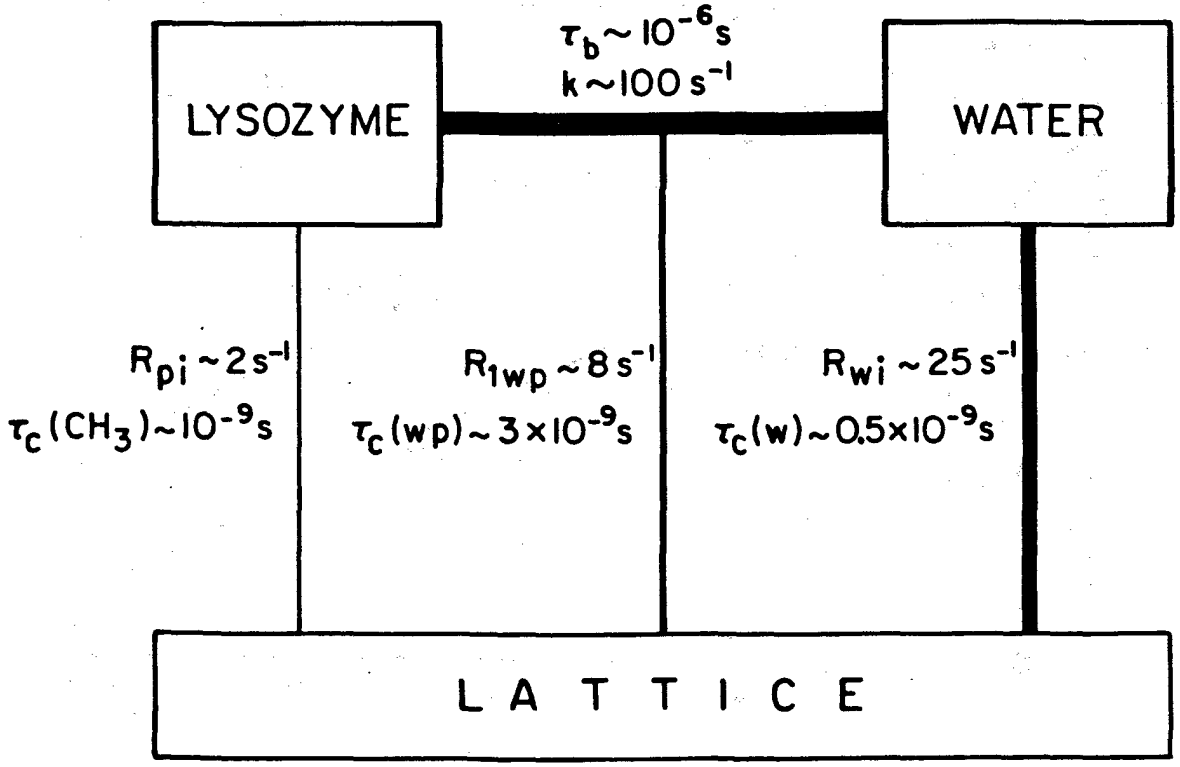

Figure 6. Relaxation model for hydrated lysozyme. τ_b is the correlation time characterizing the motion giving rise to k whereas τ_c(wp) characterizes the motion giving rise to R_{1wp}.

be possible to determine these populations from the FID. Knowledge about the $p_{a,b}$'s allows us to express k_b in terms of k_a (see eqn. 7). Then, values of $C^{\pm}_{a,b}$ are calculated for a range of k_a values using eqns. 6 and 7 as well as the following expressions for the intrinsic spin relaxation rates obtained from eqn. 5.

$$R_a = \frac{1}{2}[(\lambda^+ + \lambda^-) \pm \sqrt{(\lambda^+ - \lambda^-)^2 - 4k_a k_b}] - k_a \quad (8)$$

$$R_b = (\lambda^+ + \lambda^-) - R_a - k_a - k_b \quad (9)$$

The modelled $C^{\pm}_{a,b}$, as a function of k_a, and the experimental values are displayed simultaneously on a computer screen. The system's k_a is taken as the value of k_a that provides the best correspondence between modelled and experimental magnetization fractions in all experiments. Then, R_a and R_b are determined through eqns. 8 and 9.

In cases where information about the $p_{a,b}$'s is not readily available, the correct k_a (and k_b, $p_{a,b}$'s and $R_{a,b}$'s) may be found by parameterizing, say, p_a and performing the above graphical comparison in each experiment for a range of values of the population – until an acceptable correspondence between modelled and experimental $C^{\pm}_{a,b}$'s is found in all experiments.

In the last step of spin grouping and exchange analysis the set of model parameters that correctly predicts the results of all experiments, is used to analyse the system for molecular dynamics.

NMR spin grouping and exchange analysis has recently been applied (9, 13) to NaDNA paracrystals with hydration levels ranging from about 3 H_2O molecules to 14 H_2O molecules per nucleotide. This work involved T_2, HH T_1, SH T_1, SS T_1 and $T_{1\rho}$ experiments performed as a function of temperature and frequency. Spin grouping and exchange analysis was applied to experimental results in each case. In addition, relaxation measurements on water deuterons were performed.

Figure 7 depicts the possible hydration sites of NaDNA (14, 9). In the following we consider relaxation at 40 MHz and 6°C in the sample hydrated to the 3 H_2O molecules/nucleotide level for which essentially all the water molecules of hydration bind at the ionic phosphate site (site 1 of Fig. 7) (9). Sites 2-5 are filled as more water is added. Upon a

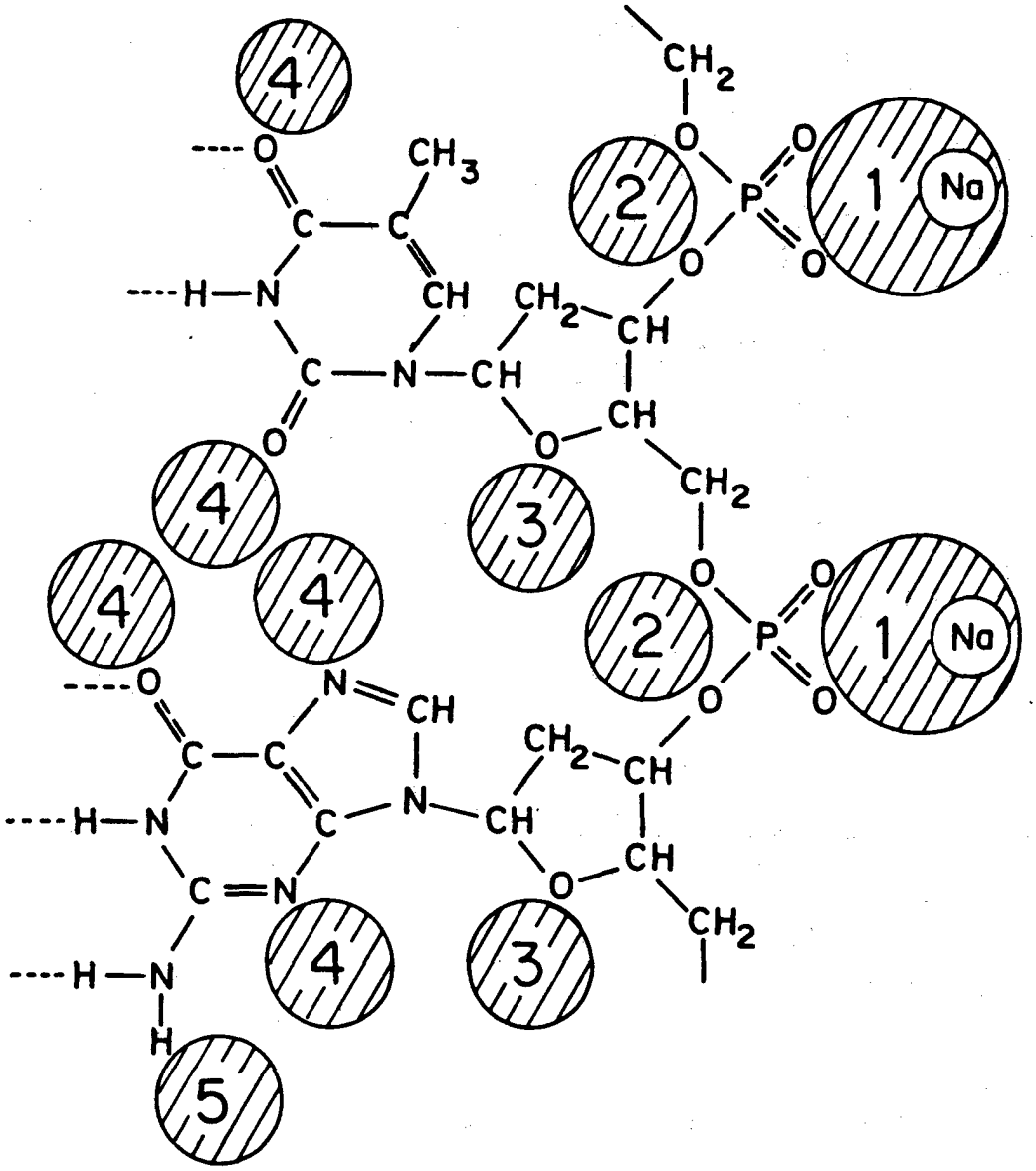

Figure 7. NaDNA hydration scheme.

HH excitation the 3 H_2O/nucleotide sample relaxes with a single T_1. FID analysis gives spin fractions of water ($\sim$ 35%, $T_2 \sim 250$ μs) and DNA ($\sim$ 65%, $T_2 \sim 12$ μs),identical to their stoichiometric values. However, upon a SH excitation ($t_p = 200\mu s$ for the S-pulse), the system relaxes with two characteristic relaxation times (9). Figure 8 gives the results of the spin grouping analysis for this experiment (13). For a two site exchange model, where p_a and p_b are equal to the stoichiometric water and DNA spin fractions, no reasonable corespondence between experimental and modelled apparent magnetization fractions could be found (9, 13).

The results of spin grouping applied to the $T_{1\rho}$ experiment at 7 G are shown in Figure 9 (13). These results are clearly at odds with a two site solid-water exchange scheme. The reconstructed FID of the magnetization with short $T_{1\rho}$ (Fig. 9) is decomposed (13) into a solid fraction (14%, $T_2 \sim 20$ μs) and a liquid fraction (37%, $T_2 \sim 450$ μs). The magnetization with $T_{1\rho} \sim 5$ ms appears as a solid (49%) with $T_2 \sim 14$ μs. Thus, water protons appear strongly coupled to a fraction of the DNA protons on the $T_{1\rho}$ timescale while the major fraction of the DNA protons (49% of sample protons or 78% of DNA protons) relax with a $T_{1\rho}$ of 5 ms.

In Figure 10 a linear three site exchange scheme, consistent with the above, is depicted (9). The α– and β–protons make up magnetizations with short and long $T_{1\rho}$, respectively. The exchange rates

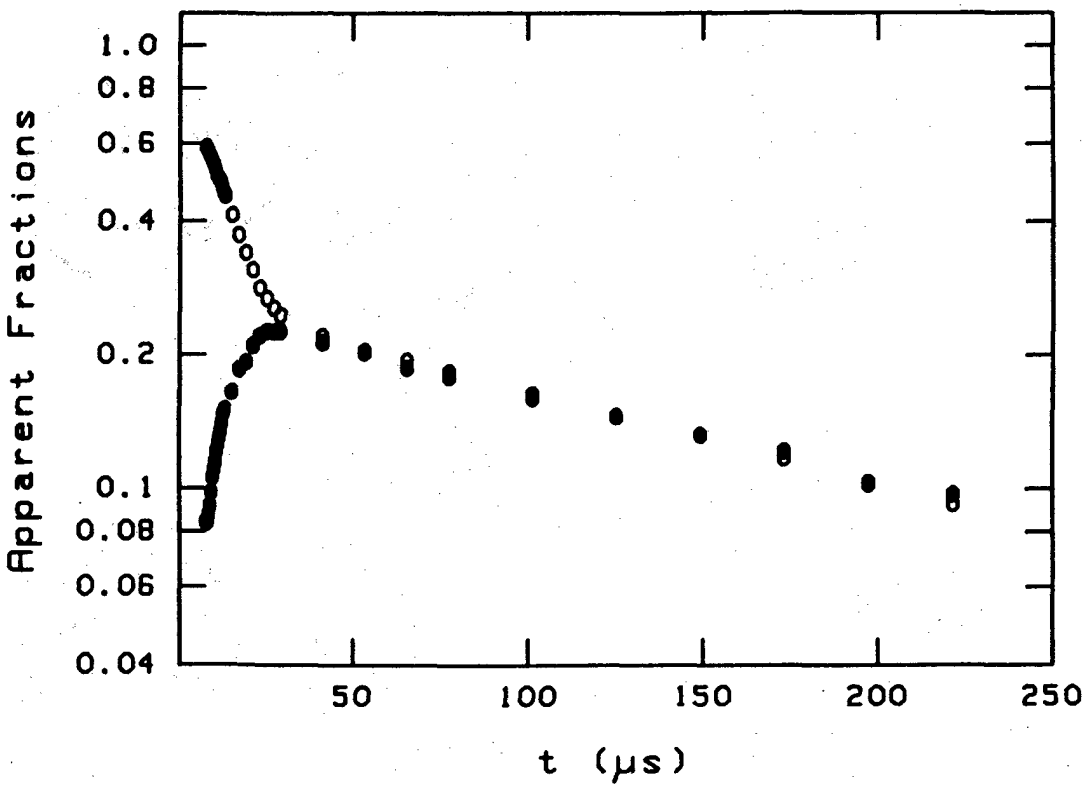

Figure 8. Apparent magnetization fractions versus t for the SH T_1 experiment in low hydration NaDNA. The filled and open circles are associated with the magnetization components with short $T_1 \sim 4$ ms and long $T_1 \sim 90$ ms, respectively.

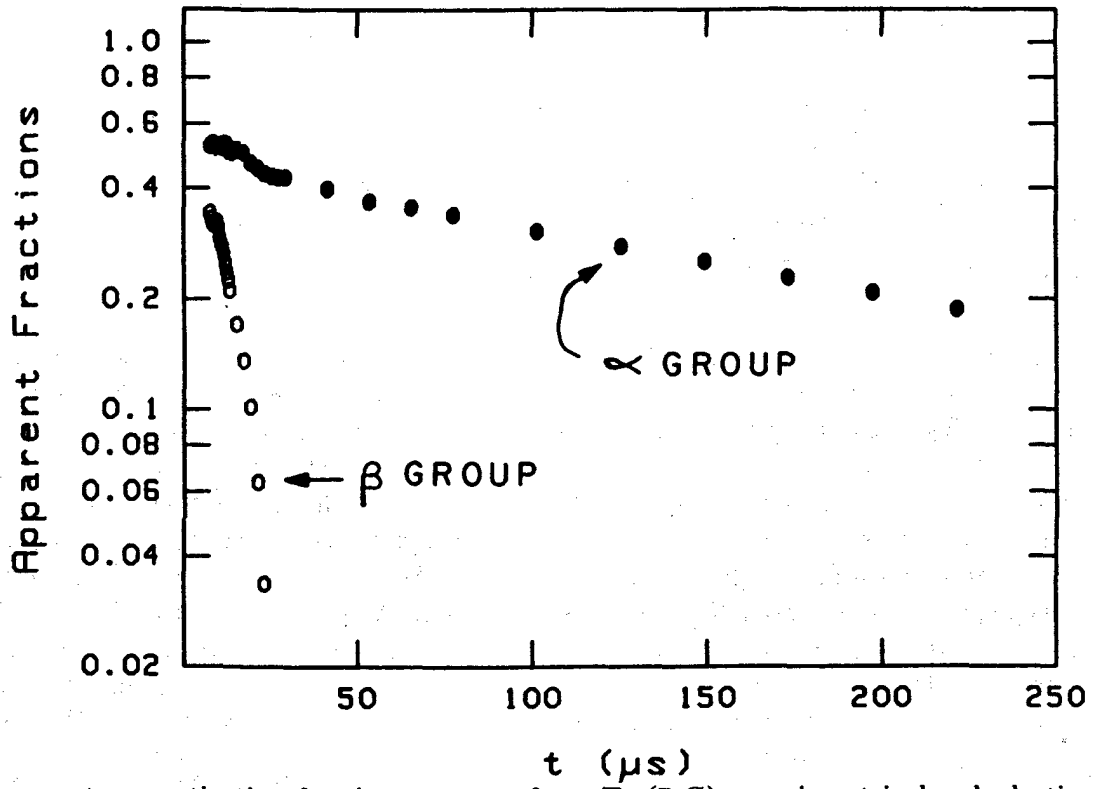

Figure 9. Apparent magnetization fractions versus t for a $T_{1\rho}$(7 G) experiment in low hydration NaDNA. The filled and open circles are associated with magnetization components with short $T_{1\rho} \sim 1$ ms and long $T_{1\rho} \sim 5$ ms, respectively.

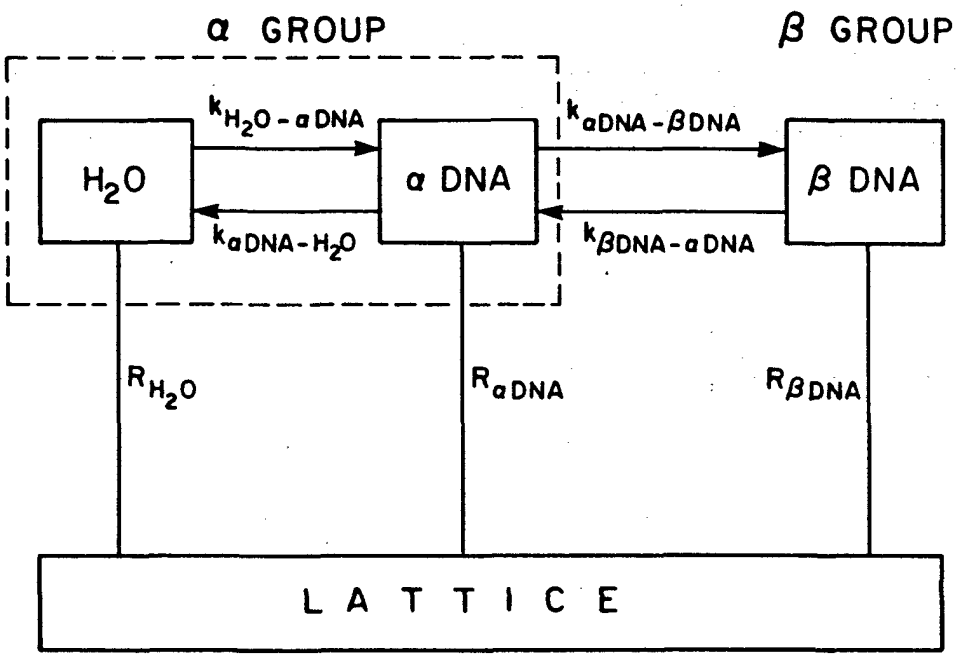

Figure 10. Three site exchange scheme for NaDNA at $3H_2O$ molecules/nucleotide hydration level.

$k_{H_2O-\alpha DNA}$, $k_{\alpha DNA-H_2O} >> T_{1\rho}^{-1}$, while the exchange between α DNA- and β DNA–protons is slow compared with $T_{1\rho}$. On the T_1 timescale, however, all exchange processes are fast. The system parameters characterizing the exchange scheme depicted in Fig. 10 were obtained (13) through the application of a three site exchange formalism in conjunction with an iterative correlation procedure. Details about the exchange analysis may be found in reference 13.

With the intrinsic relaxation parameters and exchange information obtained through the above analysis, the system was analysed for molecular dynamics (13). Anisotropic water molecule motion was found consistent with the proton and deuteron relaxation results. Although the water proton-αDNA proton intermolecular interactions produce a relatively strong spin-spin coupling ($k_{\alpha DNA-H_2O}$ $\sim$ 2300 s^{-1} at room temperature) any contribution to interfacial intermolecular proton spin-lattice relaxation was estimated to be smaller than the inaccuracy of the exchange analysis.

IV. Summary

NMR spin grouping and exchange analysis is an effective method for resolving the NMR response of a heterogeneous system. The approach consists of four steps; establishing a broad experimental basis utilizing various experimental techniques including selective excitation of spin groups, accurately detecting all apparent relaxation parameters and establishing correlations between different experiments using spin grouping, analysing the relaxation – correlation results for exchange so as to obtain intrinsic relaxation parameters, and with these data model the molecular dynamics of the system. One of the main features of this approach is that correlations among the various experiments are incorporated into the analysis. The resulting model for molecular dynamics is reliable.

Several recent applications of NMR spin grouping and exchange analysis have been reported in DNA (12 and references therein) and tissues (10, 11). In each case the resolution has been substantially improved. A study of DNA paracrystals is discussed in section III. In tissues, spin grouping and exchange analysis has been applied to determine the bulk water-bound water exchange rate [(29 ± 9) s^{-1} in mouse muscle tissue] (10).

In conclusion, the correlation spectroscopy discussed in this report provides better spin group resolution than standard pulse NMR. With this spectroscopy it is possible to determine the inherent relaxation parameters which in turn allow modeling of molecular dynamics in complex systems.

Acknowledgments

The author is thankful to Jim MacTavish for making the DNA relaxation results available for this article. Many discussions with Mik Pintar are acknowledged.

V. References

[1]J. Jeener, B.H. Meier, P. Bachmann and R.R. Ernst, *J. Chem. Phys.* **71**, 4546 (1979), and references therein.

[2]H. Peemoeller and M.M. Pintar, *J. Magn. Reson.* **41**, 358 (1980).

[3]H. Peemoeller, R.K. Shenoy and M.M. Pintar, *J. Magn. Reson.* **45**, 193 (1981).

[4]H.T. Edzes and E.T. Samulski, *J. Magn. Reson.* **31**, 207 (1978).

[5]D.E. Woessner, *J. Chem. Phys.* **35**, 41 (1961).

[6]J.R. Zimmerman and W.E. Brittin, *J. Phys. Chem.* **61**, 1328 (1957).

[7]H. Peemoeller, D.W. Kydon, A.R. Sharp and L.J. Schreiner, *Can. J. Phys.* **62**, 1002 (1984).

[8]A. Abragam, "The Principles of Nuclear Magnetism", Oxford University Press, 1961.

[9]L.J. Schreiner, Ph.D Thesis, University of Waterloo, 1985.

[10]W.T. Sobol, I.G. Cameron, W.R. Inch and M.M. Pintar, *Biophys. J.* **50**, 181 (1986).

[11]W.T. Sobol and M.M. Pintar, *Magn. Reson. Med.* **4**, 537 (1987).

[12]L.J. Schreiner, J.C. MacTavish, M.M. Pintar and A. Rupprecht, *Biophys. J.*, in press.

[13]J.C. MacTavish, Ph.D. Thesis, University of Waterloo, 1988.

[14]M. Falk, K.A. Hartman and R.C. Lord, *J. Am. Chem. Soc.* **85**, 387 (1963).